J. Membrane Biol. 111, 155–168 (1989)

The Journal of
Membrane Biology

Fatty-Acid Spin Probe Interactions with Erythrocyte Ghosts and Liposomes Prepared from Erythrocyte Ghosts

Larry M. Gordon†, Frank D. Looney‡, and Cyril C. Curtain‡

†Anesthesia Service, J.L. Pettis Veterans Administration Hospital, Loma Linda, California 92357, and ‡CSIRO Division of Biotechnology, Clayton, Victoria 3168, Australia

Summary. A model for the binding of 5-nitroxide stearate, I(12,3), to human erythrocyte ghosts was developed by comparing spin probe interactions with ghosts and liposomes prepared from ghosts. At low probe/lipid (P/L < 1/2500), I(12,3) binds to a similar class of high-affinity, noninteracting sites in both ghosts and liposomes, indicating that lipid moieties are responsible for probe uptake. Saturation occurs in both systems with increasing P/L, and, at higher loading (e.g., P/L = 1/360 for ghosts and liposomes), the probe inserts itself at initially dilute sites to form a class of low-affinity sites consisting of clusters of variable size. At still higher P/L ranges (>1/100), much increased probe uptake was observed in ghosts than in liposomes, which was attributed to another class of low-affinity sites, representing nonspecific interactions of I(12,3) with membrane proteins. The nature of the spectral components and ultrafiltration experiments with ghosts labeled at high P/L indicate that both 'dilute' and 'clustered' I(12,3) are due to membrane-incorporated probe.

Key Words erythrocyte ghosts · liposomes · radical interactions · protein · lipid domains · fluidity · electron spin resonance · spin probes

Introduction

Previous studies have shown that nitroxide radical interactions occurred in a range of biological membranes labeled with the 5-nitroxide stearate, I(12,3)[1], spin probe (for review, *see* [10, 17]). Above minimum probe/lipid (P/L) ratios (which may be as low as 1/2500), probe concentration effects similarly broaden the ESR spectra and perturb the order parameters and polarity of such diverse I(12,3)-labeled membranes as human erythrocyte ghosts [17, 19], rat liver plasma membranes [20], human platelet plasma membranes [20], human lymphocytes [11, 12], and the lipid envelope of the Human Immunodeficiency Virus (HIV) responsible for the AIDS pandemic [1, 16].

In Gordon et al. [17, 18], we presented a model for I(12,3) distribution in human erythrocyte ghosts which accurately predicted ESR spectral alterations observed with increasing P/L ratios. At low loading, I(12,3) occupies a class of high-affinity, noninteracting sites. Saturation of these sites occurs with increasing P/L, and, at higher loading, the probe inserts itself at the initially dilute sites to form a class of low-affinity sites consisting of membrane-bound clusters of variable size. The model presented in Gordon et al. [17] permitted calculation of the dilute/clustered probe ratio and showed that I(12,3) segregates in erythrocytes at relatively low P/L (e.g., 1/359). Recently, we have applied this model to quantitatively evaluate probe clustering in I(12,3)-labeled human lymphocytes [11].

Despite the success of the above membrane-bound cluster model in interpreting ESR spectral broadening in I(12,3)-labeled biological membranes, important questions remain concerning the nature of high-affinity and low-affinity binding sites in erythrocytes and other membranes. It is presently unknown whether these binding sites are due to membrane lipid or protein, or some combination of the two components. Indeed, Wallach and co-workers have presented evidence from fluorescence quenching experiments indicating that fatty-acid spin probes bind, at least partially, to the protein-lipid interface as *boundary*, or *annular* lipid [3, 40]. This interpretation would be consistent with the

[1] Abbreviations used: I(12,3), the N-oxyl-4′,4′-dimethyloxazolidine derivative of 5′-ketostearic acid; I(5,10), the N-oxyl-4′,4′-dimethyloxazolidine derivative of 12′-ketostearic acid; ESR, electron spin resonance; P/L, ratio of probe molecules to total lipid molecules; HIV, Human Immunodeficiency Virus; AIDS, acquired immunodeficiency syndrome; S, polarity-corrected order parameter; $S(T_{\parallel})$, polarity-uncorrected order parameter; $S(T_{\perp})$, polarity-uncorrected order parameter; a'_N, isotropic hyperfine coupling constant (gauss); K_a, association constant for high-affinity binding sites (mg lipid/M); N, number of high-affinity binding sites (sites/mg lipid).

general observation that I(12,3) binds not only to membrane-lipid sites as a fluid component but also to membrane-bound proteins as an immobilized component [26, 28, 29]. A distinct problem focuses on whether I(12,3), particularly at high P/L ratios where probe-probe interactions are manifest, may act as a detergent to create solubilized membrane-probe micelles. Using the technique of hygroscopic desorption, Maher and Singer [27] argued that small amphipaths such as I(12,3) would not enter biological membranes, but instead would create artifactual membrane-probe micelles.

Here, we consider the role that erythrocyte proteins play in I(12,3) binding by quantitatively contrasting the effects of a wide P/L range on the ESR spectra of I(12,3)-labeled erythrocyte ghosts and liposome extracts derived from erythrocyte ghosts. Furthermore, the possibility that I(12,3) acts as detergent-solubilizing agent at high probe loading is examined by applying the approach of Maher and Singer [27] to I(12,3)-labeled erythrocyte ghosts.

Materials and Methods

Materials

I(12,3) was obtained from Molecular Probes, Junction City, OR. Thin-layer chromatography of each batch indicated negligible impurities. Ethanolic solutions of known weight of probe were assayed for the number of paramagnetic spins per mole. Only those batches of probe assaying between 95 and 100% recovery of spins were used (*see below* and Refs. [11, 17]).

Preparation of Lipids from Human Erythrocyte Ghosts

Ghosts were isolated from human erythrocytes according to Dodge et al. [14], and lyophilized from a pH 7.4, I = 0.05, Tris-buffered suspension. Lipids were extracted by stirring 1 g of the freeze-dried powder at 20°C for 60 min in 50 ml of chloroform/methanol (70/30). The solvent was removed by evaporation in a stream of dry nitrogen for 18 hr at 20°C, and the lipid extract was stored at −20°C under nitrogen.

Preparation of Lipid Vesicles

The red cell lipids were suspended in pH 7.4, 0.05 M Tris buffer at a concentration of 100 mg lipid/ml and sonicated in an ice bath for 30 min under nitrogen. The opalescent solution was passed through a 0.2-μm filter (Nucleopore, Pleasanton, NJ). The samples were used within 6 hr of preparation. Phospholipid vesicles prepared in this way have been examined by transmission electron microscopy and have diameters ranging from 200 to 400 nm [12, 31].

Membrane Spin-Labeling and ESR Spectrometry

Stock probe solutions were prepared by dissolving I(12,3) in ethanol 3×10^{-2} M/liter. Volumes of this stock solution of less than 10 μl were dried in plastic vials under a stream of nitrogen, while larger volumes were dried *in vacuo* for 18 hr at 20°C. For lipid spin-labeling and assessment of probe incorporation, the vials for a given probe sample were prepared in sets of four. Twenty-five μl of ethanol was added to each of two vials with dried probe, and 25 μl of lipid suspension added to the other two; each vial was vortexed vigorously at 20°C for 90 sec. The contents of each vial were transferred by microsyringe to 50 μl capillary pipettes (Accufil 90 Micropets, Becton Dickinson, Parsipanny, NJ) which had been heat-sealed at one end. The extent of spin probe incorporation was calculated by comparing the amount of probe added to the vial (i.e., moles probe/moles lipid 'wt') with the paramagnetic spins observed in the microwave cavity (i.e., moles probe/moles lipid 'spins'). The number of spins in the sample was obtained from the ratio of the double-integrated membrane spectrum to that of the Varian strong-pitch reference (0.1% pitch with 3×10^{15} spins in 5.5 mm). Since I(12,3) is completely soluble in 100% ethanol, the recovery of spins in the ethanol-extracted probe sample was used to control the accuracy of pipeting and any probe deterioration after assays for purity. If the number of spins obtained in the two lipid samples did not agree to within 5%, the experiment was repeated. Probe/lipid (P/L) ratios were calculated by assuming that all of the lipid was phospholipid and cholesterol [14].

The ESR spectra (*see* Fig. 1) were recorded with a Varian V4502 spectrometer equipped with a Deltron (Sydney) Model DCM 20 temperature control accessory, and interfaced to a Hewlett-Packard 9825A computer through a Hewlett-Packard 3437A System Voltmeter. The system was equipped with a graphics terminal to facilitate computer manipulations of stored data. The data collection and manipulation programs were written in Hewlett Packard's HPL programming language, and copies may be obtained from the authors. The pipettes containing the samples were placed in a special holder fabricated out of Kel-F (attributed by Gaffney [15] to R. Kornberg) and obtained from J & M Specialties (San Diego, CA), and was mounted in the temperature accessory. The holder facilitates reproducible positioning of the sample in the microwave cavity and is crucial for performing accurate spectral subtractions (*see* below).

Evaluation of the Flexibility of the Lipid-Incorporated I(12,3) Probe

The following order parameters were used to assess the flexibility of the fatty-acid probe:

$$S(T_\parallel) = \tfrac{1}{2} \cdot [3(T_\parallel - T_{xx})/(T_{zz} - T_{xx}) - 1] \quad (1)$$

$$S(T_\perp) = \tfrac{1}{2} \cdot [3[(T_{zz} + T_{xx}) - 2T_\perp]/(T_{zz} - T_{xx}) - 1] \quad (2)$$

$$S = (T_\parallel - T_\perp) \cdot (a_N)/(T_{zz} - T_{xx}) \cdot (a'_N). \quad (3)$$

$T_\parallel$ and $T_\perp$ for the incorporated probe were determined from the ESR spectrum as in Fig. 1, and are the hyperfine splitting elements parallel and perpendicular to z', the symmetry axis of the effective Hamiltonian (H'), while T_{xx} and T_{zz} are the splitting elements of the static interaction tensor (T) parallel to the static Hamiltonian (H) principal nuclear hyperfine axes x and z. Elements of T were assessed by incorporating probe into host crystals: $(T_{xx}, T_{zz}) = (6.1, 32.4)$ gauss [10], and a_N and a'_N are the

Table 1. Hyperfine splittings, order parameters, isotropic hyperfine coupling constants, and the occupancy and association constants for high-affinity binding sites for I(12,3)-labeled human erythrocyte ghosts and liposome extracts at 37°C

Membrane systems[a]	$T_{\parallel}$[b] (G)	$T_{\perp}$[b] (G)	$S(T_{\parallel})$[c]	$S(T_{\perp})$[c]	S[c]	a'_N[d] (G)	N[e] (sites/mg lipid)	K_a[f] (mg lipid/M)
Erythrocyte ghosts	27.49	9.76	0.720	0.583	0.640	15.7	0.9×10^{15}	5.2×10^{9}
Erythrocyte ghost lipids	27.12	10.15	0.699	0.538	0.607	15.8	1.2×10^{15}	11.6×10^{9}

[a] Human erythrocyte ghosts and liposomes prepared from lipid extracts of erythrocytes were labeled with I(12,3) at probe/lipid ratios of 1/4600 [17] and 1/2500, respectively (*see* Materials and Methods).
[b] $T_{\parallel}$ and $T_{\perp}$ were measured from ESR spectra as shown in Fig. 1; $T_{\perp}$ was corrected by the addition of 0.8 G.
[c] $S(T_{\parallel})$, $S(T_{\perp})$ and S were respectively calculated from Eqs. (1), (2) and (3).
[d] a'_N, the isotropic hyperfine coupling constant, is equal to $\frac{1}{3}(T_{\parallel} + 2T_{\perp})$.
[e] N, the number of high-affinity binding sites, were determined from a distribution-free analysis of the initial portions (i.e., μg I(12,3)/mg lipid 'spins' of 1.5 for liposomes and 1.3 for erythrocyte ghosts) of the Scatchard plots (*see* Fig. 3*B*) following the methodology of Crabbe [9].
[f] K_a, the association constants for high-affinity binding sites, were determined from a distribution-free analysis of the initial portions (i.e., μg I(12,3)/mg lipid 'spins' of 1.5 for liposomes and 1.3 for erythrocyte ghosts) of the Scatchard plots (*see* Fig. 3*B*) following the methodology of Crabbe [9].

isotropic hyperfine coupling constants for the probe in membrane and crystal [i.e., $a'_N = \frac{1}{3}(T_{\parallel} + 2T_{\perp})$ and $a_N = \frac{1}{3}(T_{zz} + 2T_{xx})$]. Increases in a'_N indicate a more polar environment.

If experimentally-determined low probe concentrations are used [33], S, $S(T_{\parallel})$ and $S(T_{\perp})$ are sensitive to membrane fluidity (or, more accurately, the flexibility of the incorporated probe). These order parameters may assume values between 0 and 1, with the extremes indicating that the probe samples fluid and immobilized environments, respectively. S, which requires both splittings, corrects for small polarity differences between the membrane and reference crystal. Although $S(T_{\parallel})$ and $S(T_{\perp})$ do not include polarity corrections, these expressions are useful fluidity approximations, within certain limitations [10, 11, 21].

Determination of Nitroxide-Radical Interactions in Liposomes Using Empirical Parameters

The extent of probe-probe interactions in spin-labeled liposomes was estimated using four empirical parameters previously employed with I(12,3)-labeled biological membranes. The first measures the peak-to-peak linewidth of the central band (i.e., ΔH of Fig. 1),

$$\Delta H = \Delta H_0 + \Delta H_{dip} + \Delta H_{ex} \tag{4}$$

where ΔH_0 is the linewidth without interactions, ΔH_{dip} is the line broadening caused by magnetic dipolar interactions and ΔH_{ex} is contributed by spin-spin exchange [10]. Enhanced nitroxide radical interactions increase ΔH [34].

The second and third parameters are based on the finding that $T_{\perp}$, but not $T_{\parallel}$, broadens with increasing probe concentration in various membranes, including erythrocyte ghosts [11, 17, 19]. For those P/L ratios where the percent change in $S(T_{\parallel})$, $\Delta S(T_{\parallel})$, is zero, decreases in $S(T_{\perp})$ denote enhanced probe-probe interactions. Another way to indicate this relationship is through the m parameter [12, 17, 33].

$$m = \frac{(T_{\parallel} - a'_N)}{(T_{\parallel} - a_N)}. \tag{5}$$

Should the polarity of the membrane (a'_N) be identical to that of the reference host crystal and probe interactions are absent, then $m = 1$. However, if radical interactions increase $2T_{\perp}$, then m will decrease below 1.

The fourth measure depends on the height of the high-field peak of the inner hyperfine doublet (h_{-1} in Fig. 1) decreasing with respect to that of the central line (h_0): h_{-1}/h_0 declines as the P/L increases [10, 22].

Results and Discussion

Flexibility of the I(12,3) Probe in Human Erythrocyte Ghosts and Liposomes Prepared from Erythrocyte Ghosts

The ESR spectrum of I(12,3)-labeled liposomes prepared from the lipid extracts of human erythrocyte ghosts at a low P/L of 1/2500 (Fig. 1) indicates that the probe executes rapid anisotropic motion about its long molecular axis at 37°C. Comparison of the lipid spectrum (Fig. 2*B*) with that obtained from I(12,3)-labeled erythrocyte ghosts (Fig. 2*A*) shows that the probe exhibits more flexibility in liposomes at 37°C. The outer splitting, $2T_{\parallel}$, for the lipid spectrum is narrower than the ghost spectrum in Fig. 2, while the inner splitting, $2T_{\perp}$, is broader, indicating that the probe mobility is greater in the liposomes. Consistent with this is the finding that the h_{-1}/h_0 ratio is larger in the lipid spectrum, indicating more rapid anisotropic rotation about the long molecular axis of the probe when I(12,3) resides in liposomes.

The order parameters for I(12,3)-labeled erythrocyte ghosts and liposomes confirm the above qualitative observations (Table 1). All three order

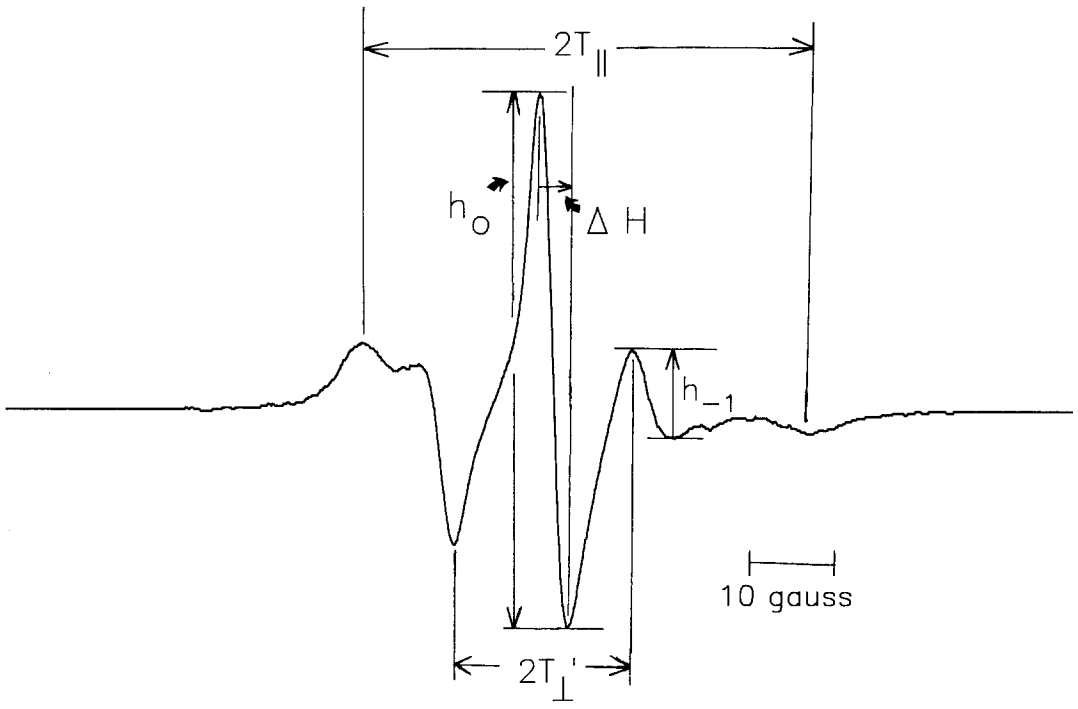

Fig. 1. ESR spectrum of I(12,3)-labeled human erythrocyte ghost lipids at 37°C, recorded using a Varian V-4502 spectrometer with a 5-min scan time, 400 receiver gain, 2 gauss modulation amplitude, 10 mW microwave power, and 0.51 sec time-constant. Outer and inner splittings, $2T_{\parallel}$ and $2T_{\perp}$ were measured as shown; $2T_{\perp}$ was corrected by addition of 1.6 gauss [21]. The peak-to-peak distance of the central line (ΔH) is shown. Heights for the central line (h_0) and the high-field peak of the inner hyperfine doublet (h_{-1}) are indicated. The P/L ratio, determined from the number of paramagnetic spins in the spectrum [11, 17], was 1/2,500

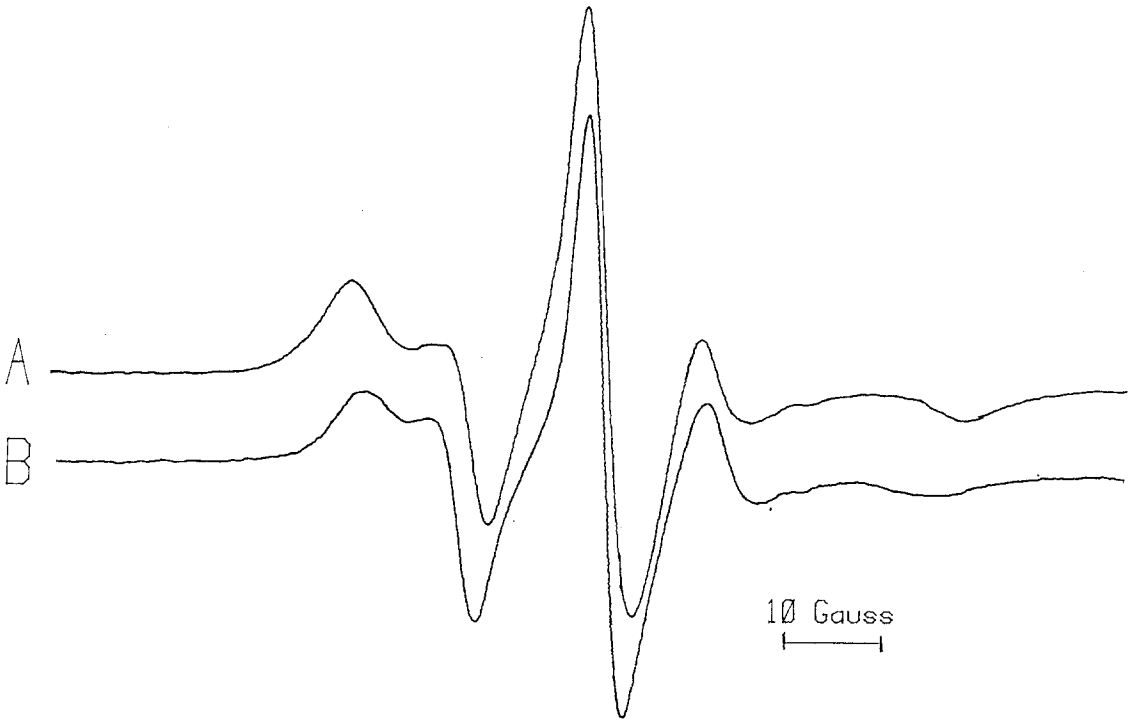

Fig. 2. ESR spectra of I(12,3)-labeled human erythrocyte ghosts (*A*) and liposomes prepared from lipid extracts of human erythrocyte ghosts (*B*). The heights of the central lines (h_0) for each spectrum are normalized. The respective P/L ratios for the membrane and lipid spectra were 1/850 and 1/810, and were calculated from the paramagnetic spins in the spectrum (*see* Materials and Methods)

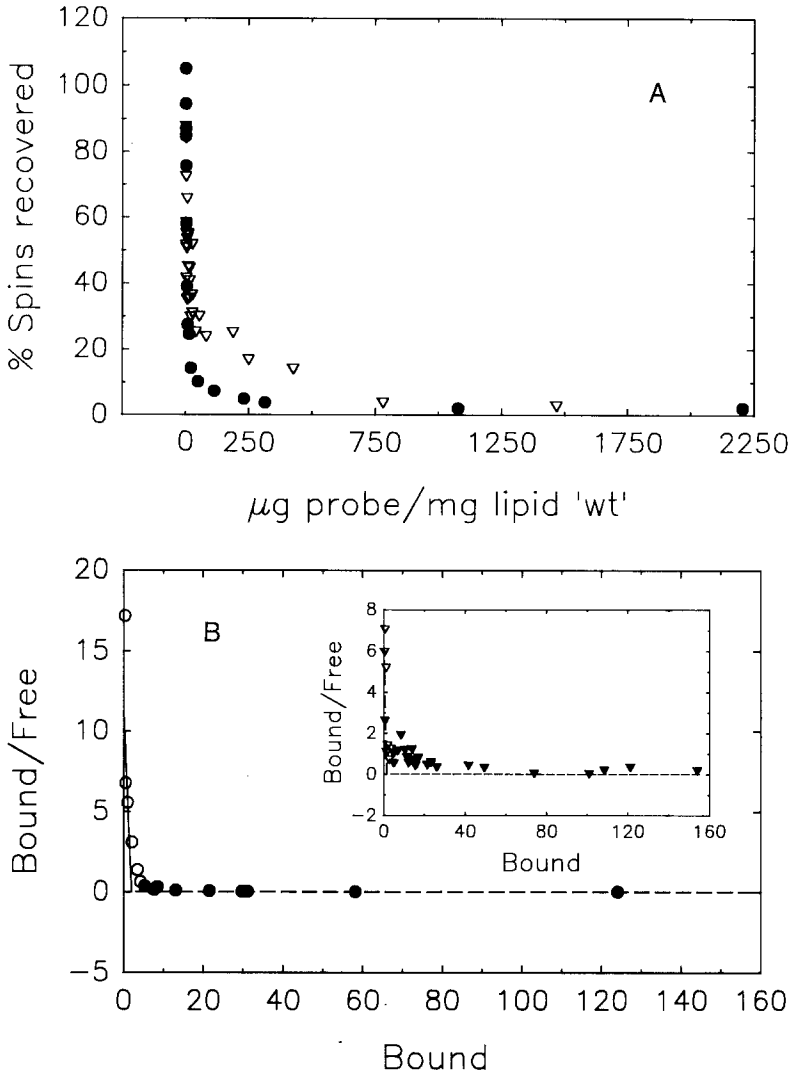

Fig. 3. I(12,3) uptake by human erythrocyte ghosts and liposome extracts from human erythrocyte ghosts. (*A*) Plot of percent recovered spins *vs.* weight of probe added to 25 μl aliquots of human erythrocyte ghosts (▽) or liposomes of lipid extracts from human erythrocyte ghosts (●). Percent recovered spins were calculated from the ratio of probe weight added to the sample (i.e., μg probe/mg lipid 'wt') to that determined from the spins in the spectra (i.e., μg probe/mg lipid 'spins'). The human erythrocyte ghost data was adapted from Gordon et al. [17]. (*B*) Scatchard plot of the I(12,3) probe uptake by liposome extracts (○; ●), where *Bound* = (nm probe/mg lipid 'spins') and *Free* = (nm probe/mg lipid 'wt' − nm probe/mg lipid 'spins'). Open circles (○) denote I(12,3) concentrations (<3.9 nm I(12,3)/mg lipid 'spins' or 1.5 μg I(12,3)/mg lipid 'spins') used to calculate the initial binding of probe to liposomes (*see text*). *Inset*: Scatchard plot of I(12,3) uptake by human erythrocyte ghosts (▽; ▼), where *Bound* = (nm probe/mg lipid 'spins') and *Free* = (nm probe/mg lipid 'wt' − nm probe/mg lipid 'spins'). Open inverse triangles (▽) denote I(12,3) concentrations (<3.4 nm I(12,3)/mg lipid 'spins' or 1.3 μg I(12,3)/mg lipid 'spins') used to calculate the initial binding of probe to erythrocyte ghosts (*see text*). Data adapted from Gordon et al. [17]. (*See* Materials and Methods)

parameters, $S(T_\parallel)$, $S(T_\perp)$ and S, are significantly lower in I(12,3)-labeled liposomes, showing that the probe samples a more fluid environment in liposomes than in ghosts. The flexibility of I(12,3) in liposomes at 37°C is similar to that determined from ESR spectra of I(12,3)-labeled erythrocyte ghosts recorded at approx. 42–43°C. Interestingly, the polarity of the probe milieu, as indicated by a'_N, is nearly identical in both liposomes and ghosts (Table 1).

Spin-Labeling of Erythrocyte Ghosts and Liposomes from Erythrocytes

I(12,3) uptake into erythrocyte liposomes was studied by contrasting the weight of the probe added to the sample (i.e., μg probe/mg lipid 'wt') to that calculated from the spins present in the ESR spectra (μg probe/mg lipid 'spins') (*see* Materials and Methods). Figure 3*A* indicates that there is quantitative uptake of I(12,3) by liposomes at low loading. However, progressively decreasing amounts of additional I(12,3) became incorporated for μg probe/mg lipid 'wt' ratios greater than 0.14.

It is important to ascertain the physical basis for the apparent "loss of spins" with increasing probe concentration in liposomes (Fig. 3*A*). Since enhanced probe-probe interactions paralleled the decrease in recovered paramagnetic spins (*see below*), studies were conducted to determine whether the loss of spins was the direct result of dipolar broadening between interacting probe molecules. Experiments to control for this phenomenon are necessary, because previous investigators have shown that such dipolar broadening may decrease signal intensity without any marked broadening of the spectrum [2, 13, 38]. Here, liposome samples (P/L 'spins' ratios > than 1/60) exhibiting radical-broad-

Table 2. Recovery of excess I(12,3) that does not incorporate into erythrocyte liposomes at high spin probe loading[a]

	Wash number					
	0[b]	1	2	3	4	5
Probe recovered (μg I(12,3)/mg lipid 'spins')	78.4	49.1	77.4	65.6	83.5	73.1
% Total probe recovered per wash	16.0	10.0	15.8	13.4	17.0	14.9

[a] Erythrocyte ghost liposomes (25 μl of 100 mg liposome/ml) were labeled with a high I(12,3) concentration (*see* text for labeling conditions), then the spin-labeled lipid sample was removed from the test tube and the tube was washed five times with unlabeled liposome samples (i.e., 25 μl of 100 mg liposome/ml per wash). The total amount of probe added to the initial lipid sample was 490 μg I(12,3)/mg lipid 'wt', while the μg I(12,3)/mg lipid 'spins' were those calculated from the double-integration of the ESR spectra for the liposome sample and washes (*see* text for definition of terms).

[b] Probe incorporated into the initial erythrocyte ghost liposome sample.

ened spectra were mixed with 10 volumes of ethanol, and the narrow-line, isotropic spectra of the solubilized probe were recorded and double-integrated. The number of spins found in the solubilized spectra ranged from 103–107% of those measured in the original liposome spectra. Thus, the apparent loss of spins noted at high P/L ratios in Fig. 3*A* was not simply due to enhanced dipolar broadening effects.

The most likely explanation for Fig. 3*A* is that liposomes have only a limited capacity for solubilizing I(12,3) at high loading. This was verified by aspirating a liposome sample (25 μl) labeled with 490 μg I(12,3)/mg lipid 'wt', and then washing the presumably empty vial five times with unlabeled liposome samples (i.e., 25 μl of 100 mg liposome/ml per wash). The μg probe/mg lipid 'spins' for labeled and successively unlabeled samples shown in Table 2 confirm that quantitative incorporation does not occur at high loading. Instead, excess I(12,3) remains as a deposit on the side of the tube.

I(12,3) probably binds to erythrocyte liposomes at specific membrane sites. Certainly, a Scatchard plot (Fig. 3*B*) shows that I(12,3) interaction with liposomes is not a simple partitioning phenomenon of an infinitely-dilute solute in an ideal solvent. For low levels of bound probe ($<$1.5 μg I(12,3)/mg lipid 'spins'), the Scatchard relationship is essentially linear and an apparent association constant (K_a) may be calculated for a class of high-affinity sites (Table 1). However, Klotz [25] has emphasized the inherent error of determining the number of high-affinity binding sites (N) from extrapolations of such plots to the abscissa. To surmount this difficulty, a distribution-free computer method [9] was employed to calculate N for the initial part of the plot which does not rely on estimates of intercepts on axes (Fig. 3*B*; Table 1). At loading higher than 1.5 μg I(12,3)/mg lipid 'spins', the I(12,3) binding isotherm shows dramatic curvature, indicating that additional probe uptake is much reduced. Several explanations may be invoked to account for this behavior. On the one hand, I(12,3) may bind to two classes of independent liposome sites (i.e., "low" and "high" affinity sites). On the other hand, probe-membrane sites when occupied at high loading may act, possibly through a cooperative mechanism, to inhibit further I(12,3) uptake. Unfortunately, examination of only Fig. 3 will not discriminate between these two models for probe-membrane interaction.

Comparing the liposome-probe uptake curve with that obtained earlier using I(12,3)-labeled erythrocyte ghosts (Fig. 3*A*) shows that quantitative incorporation into ghosts also occurs only at low probe concentrations. Above approximately 0.2 μg I(12,3)/mg lipid 'wt', markedly less additional probe is introduced into the cavity. As with I(12,3)-labeled liposomes, distribution-free analysis of the Scatchard plot revealed the existence of a class of high-affinity sites (Table 1). The number of sites is ~30% higher in liposomes, and also the K_a is approximately twice higher in liposomes. This indicates that I(12,3) binds more strongly to slightly more high-affinity sites in liposomes than in ghosts. However, the principal discrepancy between the liposome and ghost probe uptake curves (Fig. 3*A*) appears to be for μg probe/mg lipid 'wt' ratios between 25 and 750, where the amount of probe incorporated into erythrocytes is up to eightfold higher than in liposomes.

As a working model, we propose that lipid moieties are principally responsible for high-affinity sites in both ghosts and liposomes for I(12,3). Although the polarity detected by the probe is not influenced by the absence of membrane protein, the removal of membrane protein nevertheless exerts "second-order" perturbations on these sites, such that the environment of the probe is more fluid, the number of sites is slightly elevated and the binding avidity is greater. We further suggest that, for μg probe/mg lipid 'wt' between 20 and 750, the additional binding capacity shown by ghosts (Fig. 3*A*) is due to I(12,3) binding to membrane proteins, possibly at the annular lipid level (*see* Conclusions).

Unless otherwise indicated, all subsequent probe/lipid (or μg probe/mg lipid) ratios used in the following experiments were assessed by calculating the paramagnetic spins in the spectrum.

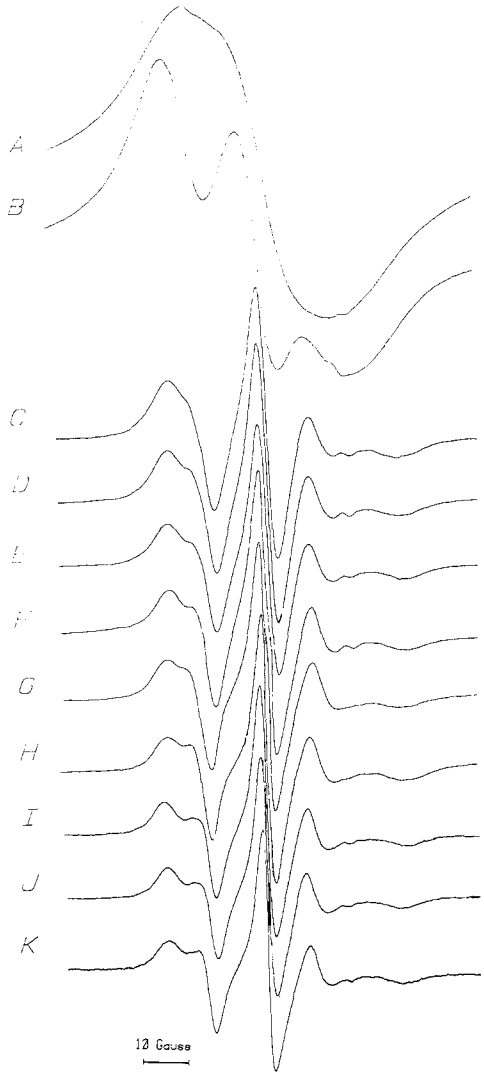

Fig. 4. ESR spectra of liposome extracts of erythrocyte ghosts at 37°C labeled with a range of I(12,3) concentrations. Lipid/probe 'spins' ratios were: (*A*) 20; (*B*) 30; (*C*) 60; (*D*) 128; (*E*) 260; (*F*) 450; (*G*) 640; (*H*) 1035; (*I*) 1490; (*J*) 2050; (*K*) 2500. Three principal P/L ranges may be defined: 'low', from 1/2500 to 1/2050; 'intermediate', from 1/2050 to 1/60; and 'very high', above 1/60 (*see text*). Figure 3*A* is defined as 'pure' phase

Effects of I(12,3) Concentration on Spectra of Liposomes from Human Erythrocyte Ghosts

The ESR spectrum of ghost liposomes labeled with a low P/L of 1/2500 (Fig. 4*K*) indicates that the probe executes rapid anisotropic motion about its long molecular axis. Since the spectrum at 1/2500 is identical to that of 1/2050 (Fig. 4*J*), a 'low' concentration range may be defined for P/L $\leq$ 1/2050. In the 'intermediate' range of 1/1490 to 1/60, raising the P/L decreased h_{-1}/h_0, displaced downward the high-field baseline and upward the low-field baseline, increased $2T_\perp$ and ΔH, and left $2T_\parallel$ unchanged (Fig. 4*C-I*). Raising the P/L above 1/60 produces a 'very high' range, characterized by noticeably broadened spectra and sloping baselines (Fig. 4*A,B*). It is not possible to reliably measure either hyperfine splittings or ΔH in this range. At these high liposome and probe concentrations, 'liquid-lines' due to I(12,3) tumbling rapidly in aqueous solution made only minor contributions (<0.5%) to the ESR spectra. Qualitatively similar spectral alterations have been reported with I(12,3)-labeled whole erythrocytes [5] or erythrocyte ghosts [17–19, 39].

I(12,3) Concentration Effects on Liposome Order Parameters and Empirical Parameters Sensitive to Radical Interactions

For 'low' P/L less than 1/2050, raising the I(12,3) concentration did not affect S, $S(T_\parallel)$ or $S(T_\perp)$. With probe concentration increases in the 'intermediate' range, however, S and $S(T_\perp)$ decreased significantly while $S(T_\parallel)$ was relatively constant (Fig. 5*A*). The most likely explanation of these order parameter effects is that they are due to enhanced radical interactions and not membrane fluidization. The broadening of $T_\perp$ [and decrease in $S(T_\perp)$] was closely correlated with decreases in m and increases in ΔH (Fig. 5*A,B*); previous studies have shown that radical interactions broaden the ΔH of labeled model and biological membranes [10, 17, 33]. Decreases in S and $S(T_\perp)$ were also correlated with such exchange-broadening consequences as the reduction in the high-field peak of the inner hyperfine doublet (h_{-1}) and the downward displacement of the high-field baseline (Fig. 4*A-I*). The observation that $T_\parallel$ [and $S(T_\parallel)$] is essentially relatively unchanged for liposomes in the intermediate range (Fig. 5*A*) indicates that the 'apparent' increase in fluidity with probe concentration, denoted by reductions in S and $S(T_\perp)$, is not the result of probe-induced perturbations; any fluidization permitting more probe mobility requires that $T_\parallel$ narrow in parallel with increases in $2T_\perp$ and h_{-1}/h_0, and that ΔH declines.

It is of interest to contrast the effects of a wide range of I(12,3) concentrations on erythrocyte liposomes with those obtained previously with erythrocyte ghosts [17, 18]. Similar to I(12,3)-labeled liposomes (Fig. 5*A*), a 'magnetically-dilute' probe concentration range was found for erythrocyte ghosts labeled with I(12,3)/lipid ratios less than 1/2250 [17]. Thus, the splittings and empirical pa-

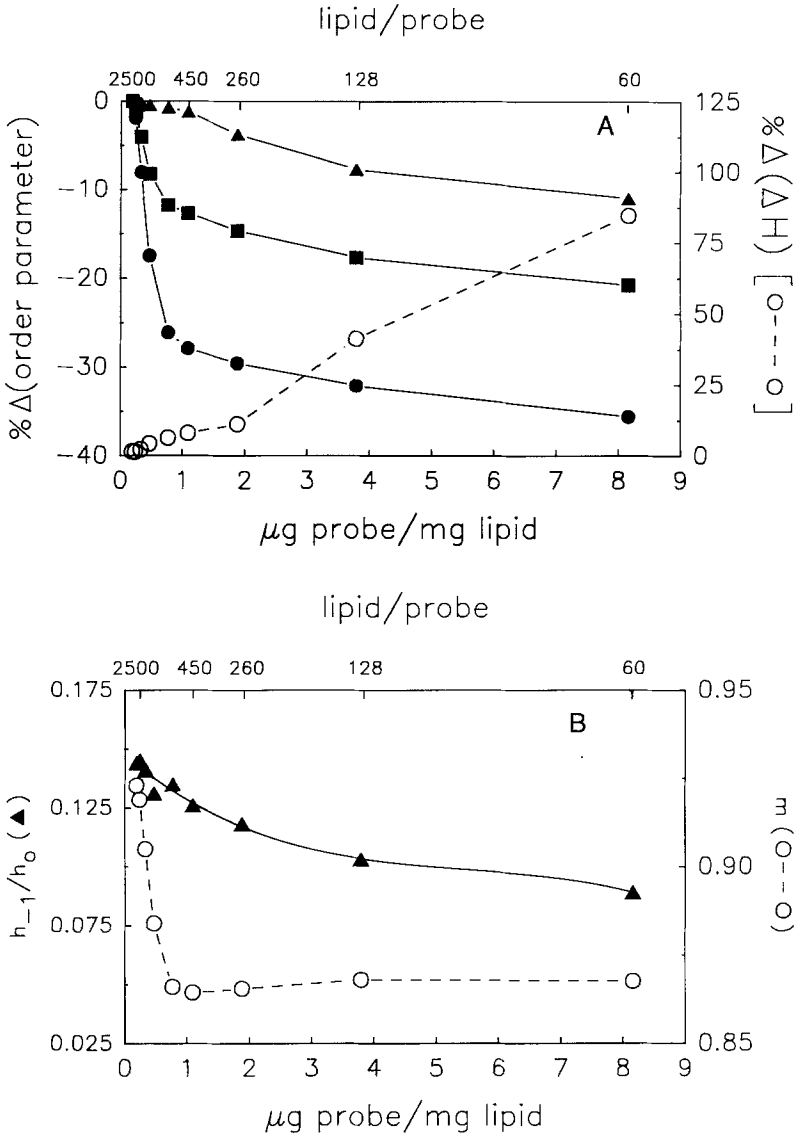

Fig. 5. Effects of increasing I(12,3) concentration in liposome extracts from human erythrocyte ghosts on order parameters and empirical parameters sensitive to probe-probe interactions. (*A*) $\Delta S(T_{\parallel})$ [▲], $\Delta S(T_{\perp})$ [●] and ΔS[■] are percent changes from baseline values measured at P/L = 1/2500. Control $S(T_{\parallel})$, $S(T_{\perp})$ and S were 0.699, 0.538 and 0.607. $\Delta(\Delta H)$ [○] are percent changes in ΔH from the baseline value of 3.6 G. (*B*) h_{-1}/h_0 as shown in Fig. 1 and m from Eq. [5]. All spectra were recorded at 37°C

rameters in Table 1 represent "intrinsic" membrane properties[2], and the order parameters accurately reflect the increased flexibility of I(12,3) in liposomes.

Equivalent I(12,3) concentration effects on order parameters and ΔH have been reported for many other biological membranes (for review, *see* Ref. [10]). Previous studies on I(12,3)-labeled erythrocyte ghosts showed that these parameters depended similarly on the probe concentration [17]. The probe effects in Figs. 4 and 5 are most probably due to enhanced ΔH_{ex} arising from I(12,3) clustering, rather than increased ΔH_{dip}. This is because the probe executes rapid anisotropic motion at 37°C and dipole-dipole interactions are relatively long-range, tending to be averaged out by rapid diffusion and/or tumbling, while exchange interactions require that labels be in van der Waal's contact and decrease rapidly with distance. A similar explanation was invoked to account for the order parameter and ΔH changes seen in I(12,3)-labeled erythrocyte ghosts with increased P/L [17].

Despite the finding that I(12,3) loading of erythrocyte ghosts or liposomes similarly affected empirical parameters sensitive to probe-probe interactions, several important differences were noted. First, comparison of the empirical parameters of Fig. 5 (*this study*) and Fig. 4 of Ref. [17] indicated that radical interactions occurred at significantly lower P/L ratios in I(12,3)-labeled liposomes; for

[2] Here, "intrinsic" properties are defined as those which are measured when probe interactions are negligible, and do not refer to membrane behavior in the absence of a perturbing label [33].

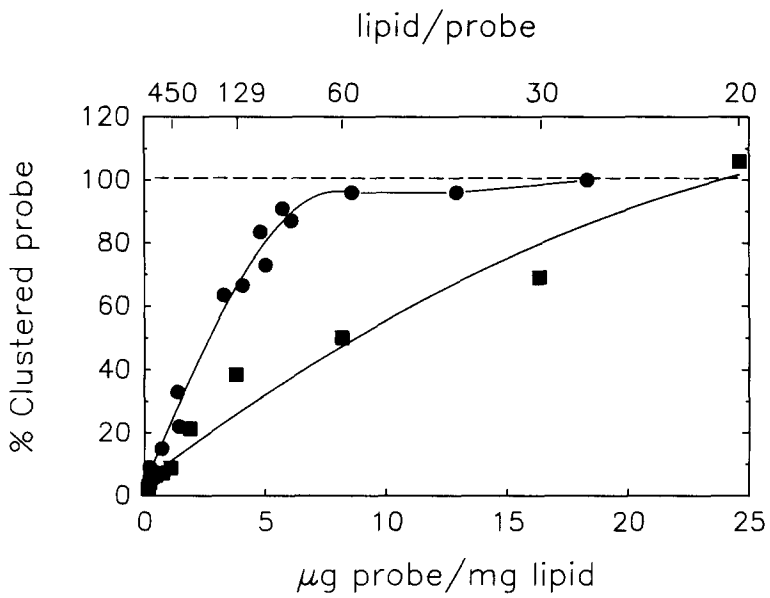

Fig. 6. Plot of the relative percentage of I(12,3) in a 'clustered' state as a function of probe concentration in either human erythrocyte ghosts [●] or liposome extracts from human erythrocyte ghosts [■]. Clustered spins in liposomes were calculated from that present in the concentrated spectrum, obtained at the titration endpoint of subtracting low-range spectrum (P/L = 1/2500) from intermediate range spectra (e.g., Figs. 7 and 8). Erythrocyte ghost data was adapted from Gordon et al. [17]

example, the $\Delta S(T_\perp)$ for erythrocyte ghosts labeled with 1 μg I(12,3)/mg lipid was −4%, while the corresponding $\Delta S(T_\perp)$ for I(12,3)-labeled liposomes was −27%. This suggests greater probe clustering in I(12,3)-labeled liposomes than in ghosts, at comparable P/L ratios. Second, for μg I(12,3)/mg lipid 'spins' greater than 4, the decline in h_{-1}/h_0 for ghosts (Fig. 4*B* of Ref. [17]) was much steeper than for liposomes (Fig. 5*B*). One possible interpretation of these data is that, for this probe range, I(12,3) binds to low-affinity sites at the protein-lipid interface. Since this binding would generate an immobilized component without a defined inner hyperfine splitting, increasing amounts of an immobilized component would sharply decrease the observed h_{-1}/h_0. This interpretation would also be consistent with our finding that ghosts bind considerably more I(12,3) than liposomes, for μg I(12,3)/mg lipid 'spins' (or μg I(12,3)/mg lipid 'wt') greater than 4 (or 25) (Fig. 3*A*).

Comparison of Probe Clustering in Erythrocyte Ghosts and Liposomes Prepared from Erythrocyte Ghosts

Since I(12,3) uptake by liposomes in the intermediate range is not due to probe binding to a single class of independent sites, Fig. 4*C–I* may be composite spectra arising from probe molecules in distinct environments. Previously, Gordon et al. [17] proposed a model for I(12,3)-labeled erythrocyte ghosts, in which similar intermediate-range spectra consisted of two components: (i) an anisotropic spectrum reflecting magnetically-dilute probe molecules occupying membrane sites; and (ii) 'concentrated' spectra that do not necessarily reflect a unique species (e.g., 'pure' phase, such as Fig. 4*A*) but instead represent variable-sized probe clusters. If exchange between these states is slow on an ESR time scale (approx. 10^{-8} sec), this model may be tested by subtracting incremental amounts of a low-range spectrum from an intermediate-range spectrum. Gordon et al. [17] showed that this yielded 'subtracted' spectra which accurately mimicked those alterations observed when I(12,3) is added experimentally to ghosts. Furthermore, relative proportions of 'dilute' and 'concentrated' probe were assessed by double integration of component spectra obtained at the subtraction endpoint. Figure 6 is a plot of % concentrated (or clustered) probe as a function of probe concentration, and shows significant I(12,3) clustering for P/L of 1/2250 to 1/359, and that, at 1/100, over 85% of the probe participates in clustering.

To determine whether this probe cluster model is also valid for liposomes prepared from erythrocyte ghosts, the subtraction protocol of Gordon et al. [17] was applied to liposomes labeled with I(12,3) concentrations in the intermediate range. The results of subtracting incremental amounts of a low-range spectrum (P/L = 1/2500) (Fig. 7*A*) from an intermediate-range spectrum (1/1490) (Fig. 7*B*) are shown in Fig. 7. The 'subtracted' spectra in Fig. 7*C–F* accurately mimic those alterations observed when I(12,3) is added experimentally to liposomes initially labeled with a P/L = 1/1490. Specifically, removing 'low' increased $2T_\perp$ and ΔH, slightly decreased h_{-1}/h_0, but left $2T_\parallel$ undisturbed. The titra-

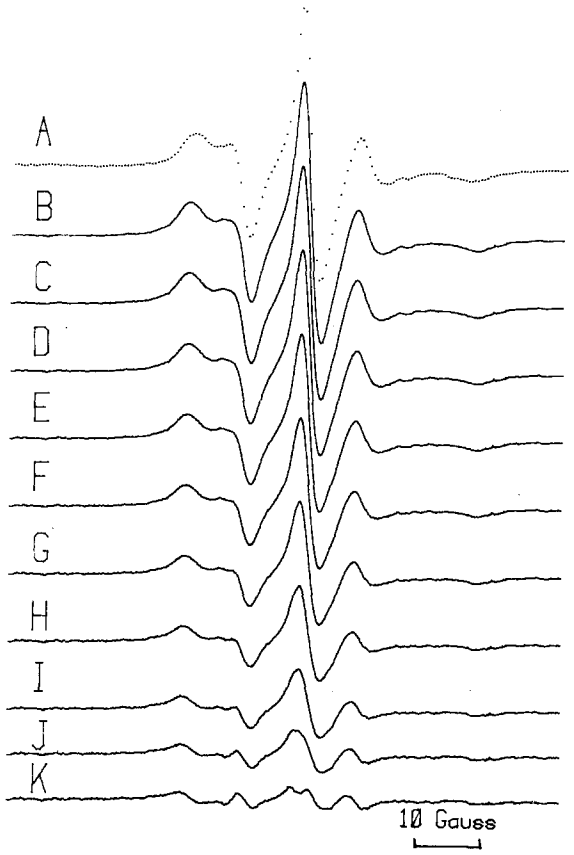

Fig. 7. Quantitation of spin probe clustering in human erythrocyte liposomes labeled with a L/P = 1490. Subtraction spectra, obtained by subtracting increasing amounts of a 'low' range spectrum (*A*) of L/P = 2500 from an 'intermediate' range spectrum of L/P = 1490 (*B*); h_0 of *B* is normalized to that of *A*. *C*, *D*, *E*, *F*, *G* and *H* are residual spectra, with double-integrated intensities of 10, 20, 30, 40, 50 and 60% of that of the unsubtracted L/P = 1490 spectrum. *I* is the spectral endpoint of the subtraction (i.e., 'concentrated' spectrum) as defined in the text. Percent 'dilute' and 'concentrated' probe are 95.8 and 4.2%, and were determined from double integration of the *B* and *I* spectra. *J* and *K* are residual spectra, with double integrated intensities of 80 and 90% of that of the unsubtracted L/P = 1490 spectrum. These are over-subtracted, as indicated by the descent of the mid-field peak. The horizontal bar indicates 10 gauss

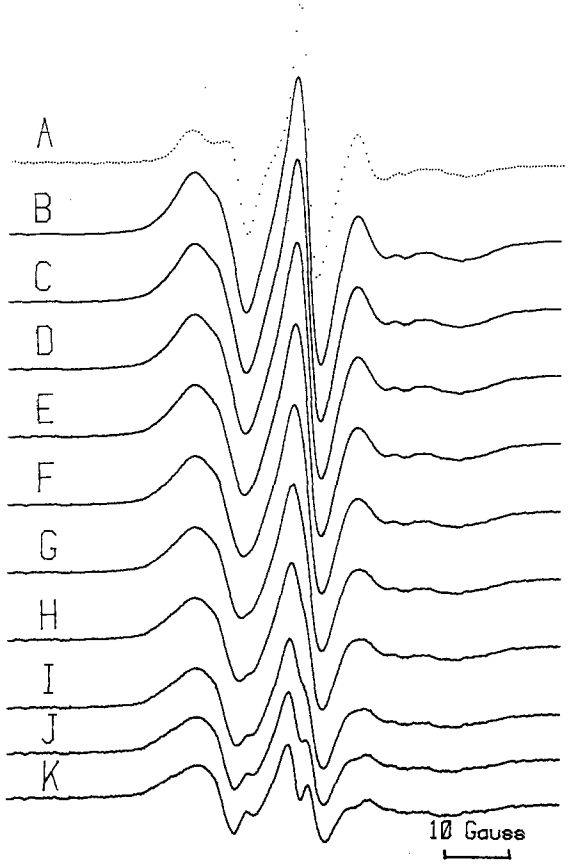

Fig. 8. Quantitation of spin probe clustering in human erythrocyte liposomes labeled with a L/P = 60. Subtraction spectra, obtained by subtracting increasing amounts of a 'low' range spectrum (*A*) of L/P = 2500 from an 'intermediate' range spectrum of L/P = 60 (*B*); h_0 of *B* is normalized to that of *A*. *C*, *D*, and *E* are residual spectra, with double-integrated intensities of 10, 20 and 30% of that of the unsubtracted L/P = 60 spectrum. *F* is the spectral endpoint of the subtraction (i.e., 'concentrated' spectrum) as defined in the text. Percent 'dilute' and 'concentrated' probe are 49.9 and 50.1% and were determined from double integration of the *B* and *F* spectra. *G*, *H*, *I*, *J* and *K* are residual spectra, with double integrated intensities of 40, 50, 60, 70 and 80% of that of the unsubtracted L/P = 60 spectrum. These are over-subtracted, as indicated by the descent of the mid-field peak

tion endpoint was indicated by the central band first becoming asymmetric and then a shoulder arising on its high-field side. These effects were due to over-subtraction such that the low-range spectrum appears in inverse phase. The 'concentrated' spectra were assigned as those immediately before central-band peak asymmetry and shoulder (Fig. 7*I*). Application of this subtraction protocol to intermediate-range spectra of liposomes at higher loading (P/L = 1/60) also produced spectral alterations (Fig. 8*C–F*) which are seen experimentally with increasing probe/lipid (Fig. 4). As the P/L ratio increased from 1/2050 to 1/20, the relative proportion of 'dilute' to 'concentrated' probe declined (Fig. 6).

Since subtracting incremental amounts of a low-range spectrum from intermediate-range spectra is a legitimate operation for I(12,3)-labeled liposomes, the probe-cluster model developed for erythrocyte ghosts [17] is also appropriate for erythrocyte liposomes. The % probe clustering curves for ghosts and liposomes each increased with increasing P/L (Fig. 6), with the liposome curve shifted to higher probe concentrations. Our observation of elevated probe clustering in erythrocytes

appears to be diametrically opposed to the findings with empirical parameters in Fig. 5, which showed greater probe-probe interactions in liposomes than in erythrocytes. The resolution of this apparent conflict lies in the nature of the 'concentrated' component in both erythrocyte ghosts and liposomes. In either system, the 'concentrated' component does not represent a unique species, but instead is due to variable-sized clusters. This is shown in the 'concentrated' spectra for P/L of 1/1490 (Fig. 7*I*) and 1/60 (Fig. 8*F*), in which the probe-probe interactions in the 'concentrated' component range from minimal to extensive. Thus, the enhanced probe-probe interactions in liposomes indicated by empirical parameters (Fig. 5) is simply due to a higher level of clustering occurring in the liposome 'concentrated' component than in the corresponding erythrocyte component, despite the dilute to clustered ratio being lower in liposomes than in erythrocyte for μg probe/mg lipid <20.

Ultrafiltration Test for I(12,3) Location in Erythrocyte Ghosts at High Probe Loading

Because of an earlier report by Maher and Singer [27] that certain amphipaths, such as chlorpromazine and decanol, may extract lipid vesicles from intact membranes, we investigated whether high concentrations of amphipathic spin probes may exert similar detergent-like effects on erythrocyte ghosts. According to this model, the clustered-probe sites would not reside in the bulk membrane, but instead be in probe-extracted vesicles exterior to it. To test this hypothesis, an ethanolic solution (100 μl) with 5×10^{15} spins of I(12,3) was added to 2.5 ml of red blood cell ghost suspension containing 10^{-7} M of lipid, and the ESR spectrum was recorded (Fig. 9*A*). Ultrafiltration of the spin-labeled ghosts was carried out following the procedure of Maher and Singer [27], using a stirred 1.5 ml Amicon (Danvers, MA) ultrafiltration cell and a 0.2 μm Nucleopore (Pleasanton, CA) hydrophobic filter. The membrane sample was first ultrafiltered, and the ESR spectra of the ultrafiltrate (Fig. 9*B*) and the residue (Fig. 9*C*), resuspended in 2.5 ml of pH 7.0, 0.05 M Tris buffer, were then recorded. The filtrate spectrum in Fig. 9*B* is dominated by the sharp triplet of I(12,3) in solution, with only a small amount of spectral broadening due to an anisotropic component characteristic of this probe in a lipid bilayer. Alternatively, the ultrafilter residue spectrum in Fig. 9*C* is very similar to the original spectrum of the unfiltered sample (Fig. 9*A*). Examination of spins recovered in the two compartments indicated 88 and 7% in the ultrafilter residue and ultrafiltrate,

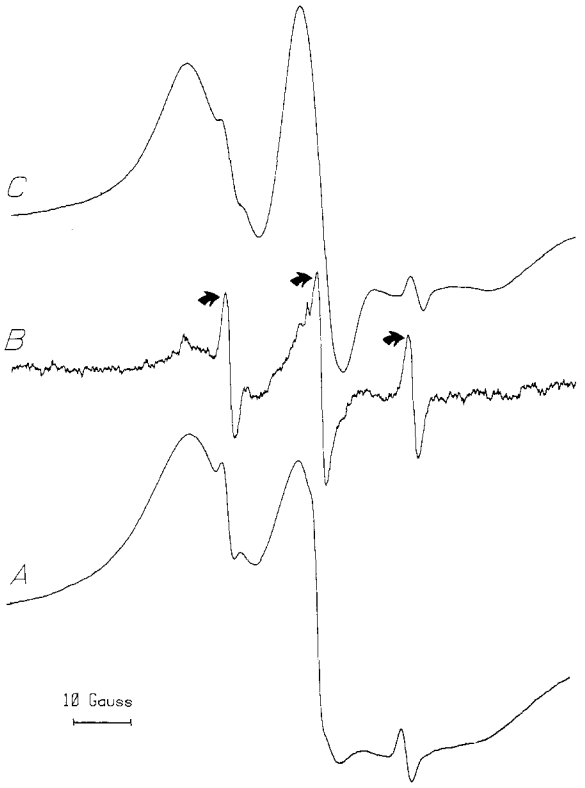

Fig. 9. Experimental test of the Maher and Singer [27] model with human erythrocyte ghosts labeled with I(12,3). (*A*) ESR spectrum of I(12,3)-labeled ghosts at a L/P of 60 ('wt') (*see* Materials and Methods); (*B*) ESR spectrum of the ultrafiltrate from the sample shown in *A*; (*C*) ESR spectrum of the ultrafilter residue from the sample shown in *A*. The 'liquid-line' component due to probe tumbling rapidly in aqueous solution is indicated by arrows. Spectra *A* and *C* were recorded at a receiver gain of 100, and spectrum *B* at a gain of 1,000. All spectra were recorded at 37°C. The % recoveries for spins in the ultrafiltrate and ultrafiltrate residue compartments (*see text*) were calculated from double integrations of *B* and *C*, with appropriate volume corrections for the ultrafiltrate and resuspended residue

respectively. Collectively, these results show that the greater part of the probe is associated with the ghosts, or fragments thereof, larger than 0.2 μm, and that it does not occur in the form of micelles of free probe or in small "probe-solubilized" membrane vesicles.

Conclusions

The above experiments permit a rigorous examination of the putative membrane-incorporation of the fatty-acid spin probe, I(12,3). Such an investigation seemed warranted, in view of the recent studies by Singer and colleagues concerning the interaction of certain amphipathic molecules with biological membranes. On the basis of hygroscopic desorption experiments, Conrad and Singer [7, 8] reported that,

although amphipaths can partition into artificial liposomes, these molecules are quantitatively excluded from internal regions of biological membranes. Specifically, the partition coefficients found for the four amphipaths, chlorpromazine, methyl chlorpromazine, 2,4-dinitrophenol and 1-decanol, exhibited partition coefficients that were at least 10^4 times higher in liposomes than in red cell ghosts [8]. Conrad and Singer [7] proposed that a large internal pressure occurred in biological membranes, but not in liposomes, such that small molecular amphipaths were excluded from the bilayer interior. Further, they suggested that amphipathic spin and fluorescent probes would also not partition into biological membranes, but instead may form concentrated micelles coating the outside of the membrane. In additional studies, Maher and Singer [27] reported that amphipaths may perturb the structure of biological membranes through "detergent-like" effects, in which vesicles are formed that are enriched in lipids and the amphipathic agent. If the Maher and Singer [27] model were applicable to erythrocyte ghosts labeled with high I(12,3) concentrations, then the broadened ESR spectra reported here would be due to micelles of membrane lipid and fatty-acid spin probe.

Our data show unequivocally that the models proposed by Singer and colleagues do not account for the interaction of I(12,3) with erythrocyte ghosts and liposomes, and that this fatty-acid spin probe incorporates into a membrane environment in both systems. Although the K_a for the high-affinity class of sites in erythrocyte liposomes is approx. 2.2 times that in ghosts (Table 1), it is far less than the 10^4 difference predicted by the Conrad and Singer [7, 8] model. Moreover, the total number of high-affinity sites (N) in ghosts is only slightly lower (~30%) than that in liposomes, whereas the Conrad and Singer [7, 8] models would forecast far fewer sites in ghosts. Our results argue against a large internal pressure existing in ghosts which prevents intercalation of the amphipathic spin probe. Further, these findings support those of Bondy and Remien [4] and Pjura et al. [30] who found no significant differences between the partitioning of small molecule amphipaths into liposomes and biological membranes using the technique of hygroscopic desorption. Pjura et al. [30] suggested that the divergent results obtained by Conrad and Singer [7, 8] might lie in their use of much higher concentrations of amphipaths (e.g., 60 μM chlorpromazine) which could produce membrane damage.

We also find no evidence for the probe "coating" the membrane surface as either probe vesicles or probe-extracted lipid vesicles. The ESR spectra for either ghosts or liposomes labeled with a "low" I(12,3)/lipid ratio indicate that the fatty acid probe incorporates into the membrane bilayer and executes rapid anisotropic motion about its long molecular axis (Fig. 2*A*,*B*). Moreover, the absence of nitroxide-radical interactions, for P/L ratios less than 1/2500 in ghosts and liposomes, precludes the existence of probe-micelles or probe-extracted lipid vesicles at low loading. Also, it should be pointed out that the high-affinity class of sites saturates at relatively low P/L ratios in both ghosts and liposomes (Fig. 3), which would not be expected if I(12,3) were to bind nonspecifically to ghosts as probe-micelles. Last, application of the hygroscopic desorption technique showed a membrane location for the majority of I(12,3) probe, even when most of the probe exists in a clustered state in erythrocyte ghosts (Figs. 6, 9).

These results allow us to revise our previous model for fatty-acid probe interactions with erythrocyte ghosts [11, 17, 19]. Since a similar class of high-affinity sites exists in both ghosts and liposomes (Fig. 3), we attribute this class of sites to lipid moieties in erythrocyte ghosts. These high-affinity sites are probably related to the class of strong binding sites detected by Shiga et al. [37] in dilution experiments of I(12,3)-labeled erythrocytes. Increasing the P/L ratio from 1/4600 to 1/359 causes probe to insert at initially dilute, lipid sites to form a class of low-affinity ghost sites consisting of clusters of variable size. Support for this interpretation comes from the similar probe-probe interaction effects noted for I(12,3)-labeled human erythrocyte ghosts [11, 17–19] and liposomes prepared from erythrocyte ghosts (Figs. 4–6). Clustering of the I(m,n) class of spin probes in lipid sites is not unexpected, as surface balance experiments showed I(5,10) clustering in mixed lipid monolayers [6] and electrophoretic mobility studies indicated I(12,3) clustering in model liposomes below the phase transition [23]. At still higher P/L ratios (>1/100), considerably more I(12,3) binds to ghosts than liposomes (Fig. 3*A*), and we attribute these results to a saturation of lipid sites as clustered probe, such that additional I(12,3) binds to lower-affinity membrane proteins as *boundary* or *annular* lipid. This model would account for the ability of fatty acid spin probes to quench the tryptophan fluorescence of ghost proteins [3, 40], although direct comparisons with this study are not possible, since Wallach and co-workers did not quantify the amount of probe binding to the membrane. Once appropriate corrections have been included for incomplete probe uptake, it would be of interest to learn if our model is correct in predicting a static component (i.e., probe

binding to protein as *annular* lipid) in Stern-Volmer plots of I(12,3) quenching of erythrocyte protein fluorescence over the same range where excess spin probe binds to ghosts.

Although the above model was developed to describe the interactions of fatty-acid spin probe with erythrocyte membranes and liposomes, it bears certain striking analogies to that proposed to account for the binding of bile salts to liposomes [35, 36]. Schubert and co-workers [35, 36] reported similar biphasic Scatchard plots for the interaction of cholate and other bile salts with model liposomes, and suggested that these agents bind to lipids with high affinity at low concentrations. At higher doses, however, where the binding of additional bile salts is hampered, they proposed that the bile salts clustered in the liposome membrane to form transient pores that could release trapped carbohydrates. It would be of considerable interest to learn whether the membrane clustering of I(12,3) observed here was similarly associated with increased bilayer permeability.

Last, it should be noted that the above probe-binding model does not provide a complete physical description for each class of sites in the erythrocyte membrane. Aside from the protein-lipid interface, these sites are most likely to be packing defects in the lipid bilayer, such as those between domain boundaries. Consistent with this hypothesis are the similarly low levels of high-affinity, probe-binding sites in either membranes or liposomes (Table 1); the number of sites/lipid molecules for erythrocyte ghosts and liposomes prepared from erythrocyte ghosts are 1/787 and 1/764, respectively. Thus, the affinity of these lipid sites for probe should be closely related to the packing properties of the probe molecule. The best approach to understanding the physical nature of the sites would be to carry out experiments with model liposomes of known composition and a range of probe molecules with differing packing properties. The ultimate goal of such studies is to develop a satisfactory physical description of the probe distribution in the membrane that permits accurate computer simulations of the ESR spectra over the entire P/L range [24, 32].

The authors thank the referees for helpful comments and Dr. R. D. Sauerheber for reading the manuscript.

References

1. Aloia, R.C., Jensen, F.C., Curtain, C.C., Mobley, P.W., Gordon, L.M. 1988. Lipid composition and fluidity of the human immunodeficiency virus. *Proc. Natl. Acad. Sci. USA* **85**:900–904
2. Altenbach, C., Hubbell, W.L. 1988. The aggregation state of spin-labeled mellitin in solution and bound to phospholipid membranes: Evidence that membrane-bound mellitin is monomeric. *Proteins Struct. Funct. Genet.* **3**:230–242
3. Bieri, V., Wallach, D.F.H. 1975. Variations of lipid-protein interactions in erythrocyte ghosts as a function of temperature and pH in physiological and non-physiological ranges: A study using paramagnetic quenching of protein fluorescence by nitroxide lipid analogues. *Biochim. Biophys. Acta* **406**:415–423
4. Bondy, B., Remien, J. 1981. Differential binding of chlorpromazine to human blood cells: Application of the hygroscopic desorption method. *Life Sci.* **28**:441–449
5. Butterfield, D.A., Whisnant, C.C., Chestnut, D.B. 1976. On the use of the spin labeling technique in the study of erythrocyte membranes. *Biochim. Biophys. Acta* **426**:697–702
6. Cadenhead, D.A., Muller-Landau, F. 1973. Pure and mixed monomolecular films of 12-nitroxide stearate. *Biochim. Biophys. Acta* **307**:279–286
7. Conrad, M.J., Singer, S.J. 1979. Evidence for a large internal pressure in biological membranes. *Proc. Natl. Acad. Sci. USA* **76**:5202–5206
8. Conrad, M.J., Singer, S.J. 1981. The solubility of amphipathic molecules in biological membranes and lipid bilayers and its implications for membrane structure. *Biochemistry* **20**:808–818
9. Crabbe, M.J.C. 1985. Distribution-free computer methods for analysing ligand binding and enzyme mechanisms. *Comput. Biol. Med.* **15**:111–121
10. Curtain, C.C., Gordon, L.M. 1984. Membrane ESR spectroscopy. *In:* Membranes, Detergents, and Receptor Solubilization. J.C. Venter and L. Harrison, editors. Vol. 1, pp. 177–213. Alan R. Liss, New York
11. Curtain, C.C., Looney, F.D., Gordon, L.M. 1987. Electron spin resonance spectroscopy in the study of lymphoid cell receptors. *Methods Enzymol.* **150**:418–446
12. Curtain, C.C., Looney, F.D., Marchalonis, J.J., Raison, J.K. 1978. Changes in lipid ordering and state of aggregation in lympocyte plasma membranes after exposure to mitogens. *J. Membrane Biol.* **44**:211–232
13. Curtain, C.C., Tosi, R., Looney, F.D. 1985. A spin label study of the ionic strength dependent conformation change in the human Ia molecule. *Molec. Immunol.* **22**:849–855
14. Dodge, J., Mitchell, C., Hanahan, D. 1963. The preparation and characterization of hemoglobin-free ghosts of human erythrocytes. *Arch. Biochem. Biophys.* **100**:119–130
15. Gaffney, B.J. 1974. Spin-label measurements in membranes. *Methods Enzymol.* **32B**:161–198
16. Gordon, L.M., Jensen, F.C., Curtain, C.C., Mobley, P.W., Aloia, R.C. 1988. Thermotropic lipid phase separation in the human immunodeficiency virus. *Biochim. Biophys. Acta* **943**:331–342
17. Gordon, L.M., Looney, F.D., Curtain, C.C. 1985. Spin probe clustering in human erythrocyte ghosts. *J. Membrane Biol.* **84**:81–95
18. Gordon, L.M., Looney, F.D., Curtain, C.C. 1987. Estimation of spin probe clustering in biological membranes. *Biochem. Biophys. Acta* **898**:202–213
19. Gordon, L.M., Mobley, P.W. 1984. Thermotropic lipid phase separations in human erythrocyte ghosts and cholesterol-enriched rat liver plasma membranes. *J. Membrane Biol.* **79**:75–86

20. Gordon, L.M., Mobley, P.W., Esgate, J.A., Hofmann, G., Whetton, A.D., Houslay, M.D. 1983. Thermotropic lipid phase separations in human platelet and rat liver plasma membranes. *J. Membrane Biol.* **76:**139–149
21. Gordon, L.M., Sauerheber, R.D. 1977. Studies on spin-labelled egg lecithin dispersions. *Biochim. Biophys. Acta* **466:**34–43
22. Gordon, L.M., Sauerheber, R.D., Esgate, J.A. 1978. Spin-label studies on rat liver and heart plasma membranes: Effects of temperature, calcium and lanthanum on membrane fluidity. *J. Supramol. Struct.* **9:**299–326
23. Hauser, H., Guyer, W., Howell, K. 1979. Lateral distribution of negatively charged lipids in lecithin membranes. Clustering of fatty acids. *Biochemistry* **18:**3285–3291
24. Humphries, G.M.K., McConnell, H.M. 1982. Nitroxide spin labels. *In:* Methods of Experimental Physics. R. Favia, editor. Vol. 20, pp. 53–122. Academic, New York
25. Klotz, I.M. 1982. Numbers of receptor sites from Scatchard graphs: Facts and fantasies. *Science* **217:**1247–1249
26. Lee, A.G. 1988. Annular lipids and the activity of Ca-dependent ATPase. *In:* Advances in Membrane Fluidity. R.C. Aloia, C.C. Curtain and L.M. Gordon, editors. Vol. 2, pp. 111–139. Alan R. Liss, New York
27. Maher, P., Singer, S.J. 1984. Structural changes in membranes produced by the binding of small amphipathic molecules. *Biochemistry* **23:**232–240
28. Marsh, D., Watts, A. 1988. Association of lipids with membrane proteins. *In:* Advances in Membrane Fluidity. R.C. Aloia, C.C. Curtain and L.M. Gordon, editors. Vol. 2, pp. 163–200. Alan R. Liss, New York
29. McNamee, M.G., Fong, T.M. 1988. Effects of membrane lipids and fluidity on acetylcholine receptor function. *In:* Advances in Membrane Fluidity. R.C. Aloia, C.C. Curtain and L.M. Gordon, editors, Vol. 2, pp. 43–62. Alan R. Liss, New York
30. Pjura, W.J., Kleinfeld, A.M., Karnovsky, M.J. 1984. Partition of fatty acids and fluorescent fatty acids into membranes. *Biochemistry* **23:**2039–2043
31. Redwood, W.R., Polefka, T.G. 1976. Lectin-receptor interactions in liposomes: II. Interaction of wheat germ agglutinin with phosphatidyl choline vesicles containing incorporated monosialoganglioside. *Biochim. Biophys. Acta* **455:**631–643
32. Rudolph, S.J. 1980. A spin-label EPR study of immunoglobulin-lipid interaction. Ph.D. Dissertation, New York University, New York
33. Sauerheber, R.D., Gordon, L.M., Crosland, R.D., Kuwahara, M.D. 1977. Spin-label studies on rat liver and heart plasma membranes: Do probe-probe interactions interfere with the measurement of membrane properties? *J. Membrane Biol.* **31:**131–169
34. Scandella, C.J., Devaux, P., McConnell, H.M. 1972. Rapid lateral diffusion of phospholipids in rabbit sarcoplasmic reticulum. *Proc. Natl. Acad. Sci. USA* **69:**2056–2060
35. Schubert, R., Beyer, K., Wolburg, H., Schmidt, K.-H. 1986. Structural changes in membranes of large unilamellar vesicles after binding of sodium cholate. *Biochemistry* **25:**5263–5269
36. Schubert, R., Schmidt, K.-H. 1988. Structural changes in vesicle membranes and mixed micelles of various lipid compositions after binding of different bile salts. *Biochemistry* **27:**8787–8794
37. Shiga, T., Suda, T., Maeda, N. 1977. Spin label studies on the human erythrocyte membrane. Two sites and two phases for fatty acid spin labels. *Biochim. Biophys. Acta* **486:**231–244
38. Taylor, J.S., Leigh, J.S., Jr., Cohn, M. 1969. Magnetic resonance studies of spin-labelled creatinine kinase system and interaction of two paramagnetic probes. *Proc. Natl. Acad. Sci. USA* **64:**219–226
39. Verma, S.P., Wallach, D.F.H. 1975. Evidence for constrained lipid mobility in the erythrocyte ghost. A spin-label study. *Biochim. Biophys. Acta* **382:**73–82
40. Wallach, D.F.H., Verma, S.P., Weidekamm, E., Bieri, V. 1974. Hydrophobic binding sites in bovine serum albumin and erythrocyte ghost proteins. Study by spin-labelling, paramagnetic fluorescence quenching and chemical modifications. *Biochim. Biophys. Acta* **356:**68–81

Received 1 February 1989; revised 17 May 1989